



Published in final edited form as:

Nat Genet. 2014 December ; 46(12): 1274–1282. doi:10.1038/ng.3129.

Common variants associated with general and MMR vaccine-related febrile seizures

Bjarke Feenstra^{1,*}, Björn Pasternak¹, Frank Geller¹, Lisbeth Carstensen¹, Tongfei Wang^{2,3,4}, Fen Huang^{2,3,4}, Jennifer L. Eitson⁵, Mads V. Hollegaard⁶, Henrik Svanström¹, Mogens Vestergaard⁷, David M. Hougaard⁶, John W. Schoggins⁵, Lily Yeh Jan^{2,3,4}, Mads Melbye^{1,8}, and Anders Hviid¹

¹Department of Epidemiology Research, Statens Serum Institut, Copenhagen, Denmark

²Department of Physiology, University of California, San Francisco, California, USA

³Department of Biochemistry and Biophysics, University of California, San Francisco, California, USA

⁴Howard Hughes Medical Institute, San Francisco, California, USA

⁵Department of Microbiology, University of Texas Southwestern Medical School, Dallas, Texas, USA

⁶Danish Centre for Neonatal Screening, Department of Clinical Biochemistry, Immunology and Genetics, Statens Serum Institut, Copenhagen, Denmark

⁷Research Unit and Section for General Practice, Department of Public Health, Aarhus University, Aarhus, Denmark

⁸Department of Medicine, Stanford University School of Medicine, Stanford, California, USA

Abstract

Febrile seizures represent a recognized serious adverse event following measles, mumps, and rubella (MMR) vaccination. We conducted a series of genome-wide association scans comparing children with MMR-related febrile seizures, children with febrile seizures unrelated to

Users may view, print, copy, and download text and data-mine the content in such documents, for the purposes of academic research, subject always to the full Conditions of use:http://www.nature.com/authors/editorial_policies/license.html#terms

*Correspondence should be addressed to B.F. (fee@ssi.dk).

URLs

Danish National Biobank, <http://www.biobankdenmark.dk/>; 1000 Genomes Project, <http://www.1000genomes.org/>; International HapMap Project, <http://www.hapmap.org/>; Ensembl browser, <http://www.ensembl.org/>; GWAS catalog, <http://www.genome.gov/gwastudies>; Genotype-Tissue Expression (GTEx) database, <http://www.ncbi.nlm.nih.gov/gtex/GTEX2/gtex.cgi>; Blood eQTL browser, <http://genenetwork.nl/bloodeqtlbrowser/>; GEUVADIS data browser, <http://www.ebi.ac.uk/Tools/geuvadis-das/>; R software, <http://www.r-project.org/>.

AUTHOR CONTRIBUTIONS

B.F., B.P., F.G., M.M., and A.H. designed the project and drafted the manuscript. B.P., H.S., M.V. and A.H. planned and performed register data acquisition, informatics, and phenotypic characterization. B.F., F.G., and L.C. carried out the statistical genetics and bioinformatics analyses. M.V.H. and D.H. performed sampling, whole-genome amplification and genotyping. J.L.E. and J.W.S. designed and performed the cell-based overexpression experiments and analysed the data. T.W., F.H., and L.Y.J. designed and performed the electrophysiology experiments and analysed the data. All authors contributed to the final manuscript.

COMPETING FINANCIAL INTERESTS

The authors declare no competing financial interests.

vaccination, and controls with no history of febrile seizures. Two loci were distinctly associated with MMR-related febrile seizures, harboring the interferon-stimulated gene *IFI44L* (rs273259; $P = 5.9 \times 10^{-12}$ vs. controls; $P = 1.2 \times 10^{-9}$ vs. MMR-unrelated febrile seizures) and the measles virus receptor *CD46* (rs1318653; $P = 9.6 \times 10^{-11}$ vs. controls; $P = 1.6 \times 10^{-9}$ vs. MMR-unrelated febrile seizures). Furthermore, four loci were associated with febrile seizures in general implicating the sodium channel genes *SCN1A* (rs6432860; $P = 2.2 \times 10^{-16}$) and *SCN2A* (rs3769955; $P = 3.1 \times 10^{-10}$), a TMEM16 family gene (*TMEM16C*; rs114444506; $P = 3.7 \times 10^{-20}$), and a region associated with magnesium levels (12q21.33; rs11105468; $P = 3.4 \times 10^{-11}$). Finally, functional relevance of *TMEM16C* was demonstrated with electrophysiological experiments in wild-type and knockout rats.

Vaccination is one of the most effective public health interventions and modern vaccines have an excellent safety record. However, on rare occasions some individuals experience serious adverse events. Investigating the underlying causes of such events is essential to maintain public confidence in vaccination and may help improve vaccine safety. Fever is a common reaction to immunization, and febrile seizures occasionally occur after vaccination, especially with live-virus vaccines such as the measles, mumps, and rubella (MMR) vaccine. Although generally well-tolerated, MMR vaccination almost triples the risk of febrile seizures in the second week following vaccination, resulting in an estimated 3 to 16 additional febrile seizure cases per 10,000 vaccinated children^{1, 2}. Overall, febrile seizures occur in 2–5% of children of European ancestry before 5 years of age³, often induced by fever from viral infections⁴.

Genetic studies of epileptic disorders with concomitant febrile seizures have identified a number of risk variants, particularly in ion channel genes^{5, 6}. However, the vast majority of children with febrile seizures do not develop epilepsy⁷, and while family and twin studies suggest a strong genetic component to isolated febrile seizures^{8–10}, little is known about specific genetic variants. It is also unknown whether distinct variants influence the risk of febrile seizures occurring as an adverse effect of MMR vaccination, or whether the MMR vaccine is just one of many possible stimuli that may trigger febrile seizures in susceptible individuals.

Here, we address these questions using a series of genome-wide association scans and replication genotyping, cell-based overexpression assays, and electrophysiological recordings of brain slices from wild-type and knockout rats.

RESULTS

Our study design is illustrated in Supplementary Figure 1. In the discovery stage, we conducted four genome-wide association scans: (1) MMR-related febrile seizures versus controls (2) MMR-related febrile seizures versus MMR-unrelated febrile seizures; (3) MMR-unrelated febrile seizures versus controls; and (4) febrile seizures overall versus controls. Sample characteristics and inclusion criteria are given in Supplementary Table 1. After imputation based on reference data from the 1000 Genomes Project, approximately 8.1 million variants were included in each of the four association scans. Genomic inflation factors were 1.01, 1.00, 1.02, and 1.03 for the four scans, respectively, indicating minimal

population stratification. Quantile-quantile and Manhattan plots are shown in Supplementary Figure 2. Based on the discovery stage results, we selected 23 SNPs representing 16 loci for replication stage genotyping (Supplementary Fig. 3). Furthermore, we conducted analyses conditioning on the selected SNPs, but no additional SNPs fulfilling the selection criteria were identified. We applied a genome-wide significance threshold of $P < 1.25 \times 10^{-8}$ since four association scans were conducted. Six independent genetic loci were replicated and reached genome-wide significance in one or more of the combined analyses (Table 1 and Supplementary Table 2).

Distinct associations for MMR-related febrile seizures

Four loci reached genome-wide significance in the analysis of MMR-related febrile seizures versus controls. Out of these, two also reached genome-wide significance in the analysis of MMR-related febrile seizures versus MMR-unrelated febrile seizures while not showing any effect in the analysis of MMR-unrelated febrile seizures versus controls (Table 1). In agreement with this, a genetic risk score based on these two loci showed no association in a logistic regression analysis of MMR-unrelated febrile seizures versus controls ($P = 0.42$) while being highly significant in comparisons of MMR-related febrile seizures versus controls ($P < 2 \times 10^{-16}$) and versus MMR-unrelated febrile seizures ($P < 2 \times 10^{-16}$). Both loci were thus distinctly associated with febrile seizures following MMR vaccination. We found no evidence of interaction between the two top SNPs. There was also no interaction between either of the two SNPs and the four SNPs for febrile seizures overall in Table 1 and their effect estimates were not changed by conditioning on the four top SNPs for febrile seizures overall (results not shown). We considered all 48 genotyped or imputed variants (SNP and indels) with $P < 1 \times 10^{-5}$ at these two loci and searched for functional predictions. These variants were all in linkage disequilibrium (LD) with the top SNP at the given locus (r^2 between 0.47 and 1; Supplementary Table 3).

At the first locus for MMR-related febrile seizures on chromosome 1p31.1, the associated SNPs fall in a sharply defined 45-kb LD block containing the gene *IFI44L* (Fig. 1a). Among 25 variants with $P < 1 \times 10^{-5}$, two were missense mutations (Supplementary Table 3). One of these, rs273259 (c.218A>G [p.His73Arg]; Ensembl transcript ENST00000370751), ranked among the lowest in P value at the locus and was selected for replication genotyping. It showed genome-wide significant association in MMR-related febrile seizures versus controls (odds ratio (OR) = 1.41, 95% confidence interval (CI) = 1.28–1.55; $P = 5.9 \times 10^{-12}$) and versus MMR-unrelated febrile seizures (OR = 1.42, 95% CI = 1.27–1.59; $P = 1.2 \times 10^{-9}$). It was not predicted to be damaging by MutationTaster or PolyPhen-2, but appears to affect relative levels of splice isoforms. The risk allele, rs273259-A, for MMR-related febrile seizures corresponds to decreased expression of exon 2 (of ENST00000370751 transcript), in which it resides, in lymphoblastoid cell lines¹¹ and corresponds to decreased expression of *IFI44L-001* (ENST00000370751) and increased expression of *IFI44L-002* (ENST00000486882) relative to other transcripts¹¹. In peripheral blood, rs273259-A is associated with decreased expression of the neighboring gene *IFI44*¹². *IFI44L* and *IFI44* belong to the group of interferon-stimulated genes (ISGs), and are both transcriptionally induced by type I interferon signaling. The expression of *IFI44L* (in dendritic cells) is significantly up-regulated following measles virus infection¹³. In a large-

scale antiviral screen of ISGs, *IFI44L* modestly inhibited hepatitis C virus replication¹⁴. We tested whether *IFI44L* impacts replication of a recombinant measles virus expressing green fluorescent protein (GFP). Using a lentiviral ectopic expression assay¹⁴, three tested *IFI44L* variants had no effect on measles virus replication in immortalized human fibroblasts lacking *STAT1* (Supplementary Fig. 4). Under these experimental conditions, *IFI44L* variants are not sufficient to confer direct antiviral protection against measles virus. Other cellular backgrounds or host factors may be important for a functional antiviral phenotype.

The most significant SNP at the second locus on chromosome 1q32.2, rs1318653 (OR = 1.43, 95% CI = 1.28–1.59; $P = 9.6 \times 10^{-11}$ versus controls and OR = 1.48, 95% CI = 1.30–1.67; $P = 1.6 \times 10^{-9}$ versus MMR-unrelated febrile seizures) lies between *CD46* and *CD34* (Fig. 1b). None of the 23 variants with $P < 1 \times 10^{-5}$ at the locus were coding, nor were they reported in the GWAS catalog or as eQTLs (Supplementary Table 3). However one of these variants, rs2724384, which is intronic in *CD46* and highly correlated with rs1318653 ($r^2 = 0.95$) has been reported in candidate gene studies to associate with immune response after MMR^{15, 16} and measles virus vaccination¹⁷. The variant rs2724384 was therefore also genotyped in the replication stage and reached genome-wide significance versus both controls and MMR-unrelated febrile seizures (Supplementary Table 2). The risk allele, rs2724384-A, for MMR-related febrile seizures corresponds to increased measles-specific IgG antibody levels^{15–17} and reduced IL-6, IFN- α , and TNF- α secretion following stimulation with vaccine-strain measles virus¹⁸. Furthermore, rs2724384-A is associated with increased expression of exons 7 and 8 of *CD46* (ENST00000358170 transcript) in lymphoblastoid cell lines as well as increased expression of *CD46-004* (ENST00000367042) relative to other transcripts and increased overall expression of the gene¹¹. *CD46* encodes a type I membrane protein that is a regulatory part of the complement system, induces proliferation and differentiation of regulatory T cells¹⁹, and acts as a cellular receptor for measles virus^{20, 21}, primarily vaccine-strain virus²².

Associations for febrile seizures in general

Variants at four loci reached genome-wide significance in the analysis of febrile seizures overall versus controls, and none of these differed between MMR-related febrile seizures and MMR-unrelated febrile seizures (Table 1 and Supplementary Table 2). A genetic risk score based on these four loci thus showed no effect in a logistic regression analysis of MMR-related febrile seizures versus MMR-unrelated febrile seizures ($P = 0.22$), but was highly significant in comparisons of MMR-related febrile seizures, MMR-unrelated febrile seizures, or febrile seizures overall versus controls ($P < 2 \times 10^{-16}$ in all three analyses). In the febrile seizures overall versus controls analysis, the 10% of children with the highest genetic risk scores were at almost 4 times higher risk than the 10% of children with the lowest risk scores (OR = 3.73, 95% CI = 3.06–4.56). We found no evidence of interaction between the four top SNPs and their effect estimates were also not changed by conditioning on the two SNPs for MMR-related febrile seizures in Table 1 (results not shown). The loci that were genome-wide significant in the febrile seizures overall versus controls analysis were also selected for genotyping in an auxiliary replication set of febrile seizures patients with 25 or more years of follow-up without any epilepsy diagnosis. Three out of four loci were replicated ($P_{\text{replication}} < 0.05$ and $P_{\text{combined}} < 1.25 \times 10^{-8}$) when using this smaller alternative

replication set (Supplementary Table 4). The febrile seizure cases in our main analysis were followed in the Danish National Patient Register until a median age of 15 years for the discovery stage cases and 10 years for the replication stage cases. In this time period 92 out of 1,999 discovery stage cases (4.6%) and 53 out of 1,443 replication stage cases (3.7%) had an epilepsy or non-febrile seizure diagnosis. We performed a sensitivity analysis excluding those cases and found very similar results compared with the main analysis (Supplementary Table 5). Next, we considered all 347 genotyped or imputed variants (SNP and indels) with $P < 1 \times 10^{-5}$ at the four loci and searched for functional predictions for these variants. Correlations with the top SNP at each locus ranged from $r^2 = 0.09$ to 1 (Supplementary Table 6).

Two loci harboring sodium channel genes

At the first locus for febrile seizures overall on chromosome 2q24.3, rs3769955 yielded the lowest P value (OR = 1.22, 95% CI = 1.15–1.30; $P = 3.1 \times 10^{-10}$). This SNP is intronic in *SCN2A* and lies in an LD block stretching into the neighboring gene *CSRNP3* (Fig. 2a). None of the 41 variants with $P < 1 \times 10^{-5}$ at the locus were coding (Supplementary Table 6), nor were they reported in the GWAS catalog or as eQTLs. *SCN2A* encodes the voltage-gated Na^+ channel alpha-subunit $\text{Na}_V1.2$, which plays an essential role in the initiation and propagation of action potentials in neurons. $\text{Na}_V1.2$ is located with high density in the axon initial segment of excitatory cortical and hippocampal neurons²³. Rare missense mutations in *SCN2A* are reported to cause benign familial neonatal and infantile seizures (BFNIS)²⁴ by a gain-of-function mechanism that increases excitability of these neurons²⁵. Furthermore, a febrile increase in temperature from 37°C to 41°C has been shown to directly increase $\text{Na}_V1.2$ channel excitability in HEK-293T cells, supporting a role for *SCN2A* in febrile seizure genesis²³.

The second locus is also on chromosome 2q24.3 in a region containing *SCN1A*, *TTC21B* and the non-coding transcripts *LOC100506124* and *LOC100506134* (Fig. 2b and Supplementary Table 6). Four SNPs at the locus were genotyped in the replication stage, all reaching genome-wide significance (Supplementary Table 2). The lowest P value was seen for rs6432860 (OR = 1.34, 95% CI = 1.25–1.43; $P = 2.2 \times 10^{-16}$), a synonymous SNP in *SCN1A* and an eQTL for *TTC21B* in the liver²⁶. Among 238 variants with $P < 1 \times 10^{-5}$ at the locus, rs7587026 was reported to associate with mesial temporal lobe epilepsy with hippocampal sclerosis with febrile seizures²⁷ in a recent GWAS meta-analysis, with the reported risk allele, rs7587026-A, corresponding to increased risk of febrile seizures in our data (Supplementary Table 6). Another associated SNP at the locus, rs3812718, affects alternative splicing of *SCN1A* in brain tissue^{27, 28}, and was significantly associated with febrile seizures in general in two relatively small sample sets, but not in a third²⁷. Again, the reported risk allele, rs3812718-A, corresponded to increased risk of febrile seizures in our data (Supplementary Table 6). *SCN1A* encodes the voltage-gated Na^+ channel alpha-subunit $\text{Na}_V1.1$, which is expressed predominantly in the axon initial segment of inhibitory interneurons²⁹. Rare mutations in *SCN1A* cause a wide spectrum of epilepsy syndromes, including genetic epilepsy with febrile seizures plus (GEFS+) and Dravet syndrome (DS, also known as severe myoclonic epilepsy of infancy)⁵, depending on the nature of the mutation and possible genetic modifiers on other genes³⁰.

In the larger region encompassing both loci, rs3769955 and rs6432860 are 660 kb apart in different LD blocks with $r^2 = 0.02$ and $D' = 0.24$ between the two SNPs based on the replication stage genotypes. Conditioning on either SNP left little residual association signal in its own LD block while only mildly attenuating the signal in the other block (Supplementary Fig. 5a,b). In an analysis conditional on both top SNPs, no SNP in the region achieved $P < 5 \times 10^{-4}$. (Supplementary Fig. 5c).

Large-effect variants at TMEM16C locus

The most significant SNP at the third locus for febrile seizures overall on chromosome 11p14.2, rs114444506 (OR = 2.09, 95% CI = 1.79–2.44; $P = 3.7 \times 10^{-20}$), lies in the first intron of the *TMEM16C* (also known as *ANO3*) splice variant *ANO3-201* (ENST00000537978) (Fig. 2c). None of the 30 variants with $P < 1 \times 10^{-5}$ at the locus were coding (Supplementary Table 6), nor were they reported in the GWAS catalog or as eQTLs. *TMEM16C* (*ANO3*) belongs to the *TMEM16* (anoctamin) protein family, a group of ten homologous transmembrane proteins that includes at least two Ca^{2+} -activated chloride channels and other members about which less is yet known³¹. Rare *TMEM16C* missense mutations have been found to segregate with autosomal dominant craniocervical dystonia and high expression of the gene in human striatum, hippocampus and cortex has been documented³². It was recently demonstrated that *Tmem16C* (*Ano3*^{-/-}) knockout rats exhibit hyperexcitability of nociceptive neurons and a decreased threshold for pain³³. Below, we investigate the potential role of *TMEM16C* in seizure genesis through electrophysiological recordings in brain slices from wild-type and knockout rats.

A locus associated with serum magnesium levels

At the fourth locus for febrile seizures overall, the top SNP, rs11105468 (OR = 1.25, 95% CI = 1.17–1.33; $P = 3.4 \times 10^{-11}$), is located in an intergenic region on chromosome 12q21.33 (Fig. 2d). All 38 variants with $P < 1 \times 10^{-5}$ at the locus were intergenic (Supplementary Table 6); none were eQTLs, but several were reported in a GWAS of serum magnesium levels, with $P = 3.8 \times 10^{-12}$ for rs11105468³⁴. For these SNPs, the allele associated with lower magnesium levels was associated with increased risk of febrile seizures in our data. It is well established that magnesium deprivation can lead to seizures in laboratory animals³⁵ and humans³⁶, and *in vitro* experiments have shown that magnesium deficiency results in spontaneous epileptiform discharges in rat hippocampal brain slices³⁷. At the molecular level, Mg^{2+} blocks the channel pore of excitatory *N*-methyl-D-aspartate (NMDA) receptors under basal conditions. The Mg^{2+} blockade is relieved by cellular depolarization thus allowing Ca^{2+} and Na^+ to enter the postsynaptic neuron as potassium exits³⁸. To explore the role of other variants associated with magnesium levels, we looked up the top SNP at all 9 confirmed and suggestive loci for serum magnesium levels³⁴, but apart from the 12q21.33 locus these loci were not associated with febrile seizures (Supplementary Table 7).

Electrophysiology, TMEM16C knockout rats

We performed electrophysiological recordings in brain slices of wild-type and *Tmem16C* knockout rats³³ to investigate potential mechanisms involving *TMEM16C* in febrile seizure genesis. Given the role of anterior hypothalamic nucleus (AHN) in thermoregulation³⁹, we

first performed whole-cell patch-clamp recordings of AHN neurons to determine the effect of *TMEM16C* on spontaneous action potential (SAP) firing patterns at different temperatures. Recordings were done in slices from postnatal day (P) 10 to 12 male rats at 33°C, 36.5°C, and 40°C, and we found a significantly lower proportion of heat sensitive neurons (increased SAP firing with increasing local brain temperature) in *Tmem16C* knockout rats compared to wild-type rats (Fig. 3, Fisher's exact test, $P = 0.005$, $n = 30$ for each group; see Supplementary Fig. 6 for the distribution and comparable membrane properties of AHN neurons from wild-type and *Tmem16C* knockout rats).

The hippocampus is often the focus of seizures; hence, we next examined whether *TMEM16C* influences hippocampal neuronal excitability. We performed whole-cell current clamp recordings of hippocampal pyramidal neurons from P14 male wild-type and *Tmem16C* knockout rats at different temperatures. Slice recordings from CA1 pyramidal neurons revealed that the resting membrane potential (V_m) is more depolarized by 4–5 mV in *Tmem16C* knock-out rats compared with wild-type controls at room temperature (Supplementary Fig. 7a, Student's t-test, $P < 0.05$, $n = 9–11$). Furthermore, current step injections revealed that neurons from knockout rats fire more action potentials than wild-type neurons at the same amount of injected current (Supplementary Fig. 7e,f). To mimic body temperature shifts in fever, we performed similar experiments at 36.5°C and 40°C and found hippocampal neurons without *Tmem16C* to display increased excitability at both temperatures (Fig. 4, two-way ANOVA, $P < 0.01$).

DISCUSSION

In this work, designed to investigate both the genetics of an adverse vaccination effect and of febrile seizures, we demonstrated that two loci were distinctly associated with febrile seizures as an adverse event following MMR vaccination and that four additional loci were associated with febrile seizures in general. Further, in the absence of *TMEM16C*, hypothalamic neurons were less responsive to heat, which could lead to impaired homeostatic control when body temperature rises, and hippocampal neurons became hyperexcitable, which could possibly contribute to febrile seizure genesis.

Our findings, implicating loci harboring the innate immune system genes *IFI44L* and *CD46*, represent a first step in understanding the biological mechanisms underlying febrile seizures as an adverse effect of MMR vaccination. An important next step will be to elucidate the pathways by which the identified variants influence the immune response and contribute to the development of fever, seizures, or both. One possibility might be that the pathogenic mechanism of MMR-related febrile seizures involves two independent steps: febrile response influenced by the distinct MMR-related febrile seizure variants, and then, given fever, seizure response influenced by the general febrile seizure variants. A genetic study of children with detailed information about febrile response after MMR vaccination would be needed to reveal if the *IFI44L* and *CD46* variants are associated with specific fever patterns also in individuals who are not susceptible to febrile seizures. Other future investigations are required to identify the precise identity of causal variants at the loci and to determine whether the variants are associated with response to other vaccines or to live virus

infections. Eventually such knowledge may translate into improved vaccine design or personalized vaccination strategies.

Concerning febrile seizures in general, *SCN1A* and *SCN2A* are strong functional candidates at the two independent 2q24.3 loci, since variants in these genes have been linked to a range of epilepsy syndromes, some involving febrile seizures^{5, 6}. Some observations are worth noting. First, variants affecting *SCN2A* function are likely to show age-dependent changes in effect, since Na_v1.2 channels are expressed early in development at the axon initial segment of principal neurons, but are gradually replaced by Na_v1.6 channels during maturation. This has been suggested as a possible explanation for the age-dependent remission of seizures in BFNIS²⁵, and might also play a role in the spontaneous remission of febrile seizures around 6 years of age, if a causal link with *SCN2A* function underlies the febrile seizure association seen in our data. Second, given the predominant expression of Na_v1.1 and Na_v1.2 channels in the axon initial segment of inhibitory interneurons and excitatory pyramidal neurons, respectively, it is conceivable that the *SCN1A* variants affect risk of febrile seizures through decreased activity of the inhibitory circuitry, whereas the *SCN2A* variants act directly by increasing the activity of excitatory neurons. Third, rare *SCN1A* missense mutations are commonly found in DS and GEFS+, two epilepsy syndromes that include febrile seizures as part of the clinical presentation. Mice that are heterozygous for *SCN1A* loss-of-function mutations show a severe phenotype resembling DS^{29, 40}, whereas mice heterozygous for GEFS+ *SCN1A* missense mutations only have partial loss of function and show a much less severe phenotype^{40, 41}. In line with this pattern, we expect future investigations to uncover more subtle effects of the *SCN1A* variants identified here on febrile seizure susceptibility, e.g., involving decreased gene expression or altered regulation of alternative splicing.

The 12q21.33 association indicates that revived research into the role of magnesium deficiency in seizure susceptibility is warranted. In clinical practice, magnesium sulphate has long been used as an effective treatment for the seizures of neonatal tetany⁴² and eclampsia⁴³, and oral magnesium supplementation has been suggested as an adjunct therapy in patients with drug resistant epileptic seizures^{44, 45}. We note that other previously reported magnesium-related loci were not associated with febrile seizures. However, these findings were based on serum concentrations measured in adult participants³⁴, and different loci may regulate different aspects of magnesium metabolism, such as tissue-specific bioavailability, over a lifetime.

The implication of *TMEM16C* variants in general febrile seizure susceptibility opens novel avenues for future research in the field of seizure disorders. Compared to typical GWAS findings in other complex diseases, the odds ratio estimate of 2.09 is unusually high, which together with the supportive electrophysiological results underline the importance of *TMEM16C* as a target for further inquiry. In nociceptive dorsal root ganglion neurons *TMEM16C* acts indirectly by modulating the properties of the sodium activated potassium (K_{Na}) channel *KCNT1* (*SLACK*)³³, but it is unclear whether this is also the case in central neurons, e.g., hippocampal and hypothalamic neurons. Rare *KCNT1* mutations have been reported in two early onset epileptic disorders^{46, 47}, and it will be interesting to determine if the mechanism underlying the association with febrile seizures reported here involves altered cellular excitability through interaction between *TMEM16C* and *KCNT1*.

Given the occurrence of febrile seizures in several epilepsy syndromes, one might speculate whether our association findings for general febrile seizures could be driven by the presence of infants who would later develop epilepsy, e.g., GEFS+ or DS. We consider this scenario highly unlikely since only a small fraction of febrile seizure cases is expected to later develop epilepsy⁷. Thus, an epilepsy variant would need to have an extremely large effect in this set and to be in strong LD with the top SNP at one of the loci for general febrile seizures in order to drive the association. However, among common SNPs at the four loci, the effect size for the only previously reported genome-wide significant epilepsy related SNP, rs7587026, was modest (OR = 1.42)²⁷, and it is implausible that rare large-effect variants in *SCN1A* and *SCN2A* known to cause familial epilepsies can explain the associations with the common SNPs (risk allele frequencies > 0.4) reported here⁴⁸. Furthermore, we found that results did not change when excluding febrile seizure cases who later developed epilepsy (Supplementary Table 5) and that three out of four loci replicated when using an auxiliary set of febrile seizure cases with more than 25 years of follow-up without any records of epilepsy (Supplementary Table 4) with the association signal for rs376995 at the last locus being consistent with the replication stage result in the main analysis (Table 1).

Our study was restricted to individuals of Danish descent, and further studies are needed to examine effects of the identified variants in populations of different ancestry. Several of the 6 SNPs in Table 1 show substantial differences in allele frequency, particularly between East Asian and other populations (Supplementary Fig. 8). The incidence of febrile seizures varies considerably in different populations across the world. In Japan, 6–9% of children experience febrile seizures compared to 2–5% in children of European descent^{3, 49}, and genetic studies in East Asian or other populations might reveal different febrile seizure loci. Further studies are also required to identify the functionally relevant variants at each locus and examine their effects in thoroughly characterized febrile seizure samples across the entire phenotypic spectrum; from isolated febrile seizures (simple or complex) to febrile seizures occurring in specific epilepsy syndromes, such as GEFS+ or DS.

In conclusion, using detailed health register information on vaccinations and febrile seizure episodes, we identified common variants at two loci associated with febrile seizures as an adverse event following MMR vaccination. From a public health perspective, it is essential to study the underlying causes of any serious adverse event of the MMR vaccine, a preventive pharmaceutical product given to millions of children each year, and our findings provide important leads for further research in the fields of immunogenetics and vaccinology. Concomitantly, we identified four loci associated with febrile seizures in general, which together with supporting evidence from electrophysiological experiments underline the importance of altered ion channel function in this common childhood disorder. Further functional studies will illuminate the biological mechanisms behind the associations reported here and might also provide more general insights into mechanisms of epileptogenesis and neuronal hyperexcitability.

ONLINE METHODS

Subjects

The cases for both the discovery and replication stages were identified from the Danish National Patient Register, which includes individual-level information from all hospitals in Denmark including physician-assigned diagnoses and dates of hospital contact⁵⁰. The register includes information on all inpatient admissions since 1977 and all emergency and outpatient hospital contacts since 1995 with diagnostic information coded according to the International Classification of Diseases (ICD, version 8 through 1993 and version 10 from 1994). The positive predictive value of a diagnosis of febrile seizures (ICD-8 and ICD-10) recorded in the register is 93%⁵¹. Information on other medical conditions was similarly obtained from the Danish National Patient Register. Data on gestational age at birth were derived from the Danish Medical Birth Register, which records detailed information on all births in the country⁵². Information on vaccination status and date of vaccination was obtained from the Childhood Vaccination Database at Statens Serum Institut⁵³. Two brands of MMR vaccine have been in use in Denmark through the period during which cases were recruited to the study. MMR II (Sanofi Pasteur MSD, Lyon, France [in the United States: Merck&Co, Whitehouse Station, NJ]) was used through October 17, 2008; this contains the Enders' Edmonston measles strain, the Jeryl Lynn mumps strain, and the Wistar RA27/3 rubella strain. From October 18, 2008, Priorix (GlaxoSmithKline Biologicals, Rixensart, Belgium) has been used; this contains the Schwarz measles strain, the Jeryl Lynn mumps strain, and the Wistar RA27/3 rubella strain. Varicella immunization is not included in the national vaccination program in Denmark. De-identified information was linked between these sources of data, which all have nationwide coverage, through the use of unique personal identifiers.

Cases for the discovery stage were identified from a background population of children born in Denmark between January 1, 1991, and December 31, 2008, with follow-up for an index event of febrile seizures between January 1, 1992, and January 1, 2010. Following identification of febrile seizure cases associated with MMR vaccination, cases of febrile seizures with no association to MMR vaccination were matched according to calendar year of index event. Cases for the replication stage were identified from a background population of children born in Denmark between January 1, 1991, and September 30, 2011, with follow-up for an index event of febrile seizures between January 1, 1992, and September 30, 2012. ICD-8 code 78021 and ICD-10 code R560 were used for case identification. A vaccine-associated case was defined as a case of febrile seizures that occurred in a risk window of 9 to 14 days following the date of MMR vaccination¹. A febrile seizures case with no association to vaccination was defined as a case that occurred 6 weeks or more after vaccination or in an infant with no vaccine exposure (the risk of febrile seizures increases transiently after MMR vaccination and is back to baseline risk by 4 weeks following vaccination^{1, 2}; our definition of cases with no association to vaccination was thus conservative with regard to the time window after vaccination). All cases were required to be between 1 and 2 years of age at the index date of the febrile seizure event, and were allowed to have experienced additional febrile seizure events either before 1 year of age or after the index event. Follow-up information from the Danish National Patient Register was

available until 11 January 2014. At the end of the follow-up period, the febrile seizure cases were between 5.1 and 23.0 years old (median 15.1 years) in the discovery stage and between 2.6 and 23.0 years old (median 10.0 years) in the replication stage. As a sensitivity analysis, we conducted association testing excluding all febrile seizure cases who had an epilepsy or non-febrile seizure diagnosis code during follow-up. Furthermore, an independent set of febrile seizure cases with 25 or more years of follow-up without any epilepsy diagnosis were included in an additional replication stage analysis.

Population controls ($n = 4,118$) for the discovery stage were selected from individuals with GWAS data from various Illumina Omni Arrays generated in other research projects at Statens Serum Institut, excluding individuals with febrile seizures or epilepsy diagnosis codes in the Danish National Patient Register. Controls for the replication stage were randomly selected among children from the Danish National Birth Cohort⁵⁴, who had participated in all surveys including the 11 year follow-up investigation, and who did not have any febrile seizure or epilepsy diagnosis code. Sample characteristics and inclusion criteria for cases and controls are shown in Supplementary Table 1.

To ensure a high degree of genetic homogeneity in the genotyped sample, we obtained birthplace information from the Civil Registration System⁵⁵, and only included subjects who were born in Denmark and whose parents and grandparents were not born outside of northwestern Europe. The study was approved by the Scientific Ethics Committee for the Capital City Region (Copenhagen) and the Danish Data Protection Agency. The Scientific Ethics Committee also granted exemption from obtaining informed consent from participants (H-3-2010-003) since the study was based on biobank material.

Sampling, Amplification and Genotyping

All samples were drawn from the Danish Newborn Screening Biobank and the Danish National Birth Cohort biobank, both of which are part of the Danish National Biobank. All cases and controls were sampled using two 3mm punches from dried blood spot samples. Genomic DNA was extracted using the Extract-N-Amp kit (Sigma-Aldrich, St. Louis, MO, USA) and then whole-genome amplified in triplicate using the Repli-g kit (Qiagen, Hilden, Germany) at Statens Serum Institut as previously described⁵⁶. All 6,117 samples in the discovery stage of the GWAS were genotyped with Illumina Omni Bead Arrays and Genome Studio software; febrile seizure cases ($n = 1,999$) were genotyped using the HumanOmniExpressExome-8 v1.1 array; controls were genotyped using the HumanOmniExpressExome-8 v1.1 array ($n = 1,931$), the HumanOmniExpress-12v1_H array ($n = 1,173$), or the HumanOmni1-Quad v1.0 ($n = 1,014$). For the replication stage, we sampled 408 cases with febrile seizures following MMR vaccination, 1,035 febrile seizure cases unrelated to vaccination, 1,647 controls and 515 febrile seizure cases with 25 years of follow-up without any epilepsy diagnosis. Genomic DNA was extracted from punches of dried blood spot samples and amplified using the same protocol as in the discovery stage. Genotyping for the selected replication stage SNPs was performed using competitive allele-specific PCR (KASP) chemistry (LGC Genomics, Hoddesdon, UK).

Data cleaning and Imputation

The data cleaning process was initiated by aligning all genotypes to the forward strand and restricting the data to the 615,786 SNPs that were available on all three different Omni arrays in the study. Next, we excluded individuals that (i) had more than 4% missing genotypes, (ii) had an autosomal heterozygosity rate deviating more than 2.5 standard deviations from the mean, (iii) had discordant sex information, or (iv) were more than 6 standard deviations away from the mean of any of the first 5 principal components in a principal component analysis. We then excluded SNPs based on a missing rate >2%, minor allele frequency <0.01, and deviations from Hardy-Weinberg Equilibrium ($P < 10^{-6}$). Finally, we excluded SNPs that showed differential missingness between arrays, differences in allele frequencies between arrays, or differences in allele frequencies between male and female subjects. The remaining 548,642 SNPs were used for imputation. We used a two-step procedure to impute unobserved genotypes using phased haplotypes from the integrated Phase I release of the 1000 Genomes Project⁵⁷. In a first pre-phasing step, we used SHAPEIT⁵⁸ to estimate haplotypes for our study samples. In a second step, we imputed missing alleles for additional SNPs directly onto these phased haplotypes using IMPUTE2⁵⁹. We chose imputed SNPs or insertion/deletions (indels) with minor allele frequencies (MAFs) of >1% and SNPTEST⁶⁰ info value of >0.8 for further analyses. Depending on the analysis, this yielded 8,129,553 (febrile seizures overall versus controls), 8,129,524 (MMR-related febrile seizures versus controls), 8,129,384 (MMR-unrelated febrile seizures versus controls), or 8,129,288 (MMR-related febrile seizures versus MMR-unrelated febrile seizures) imputed genetic variants. To further assess imputation accuracy of the six genome-wide significant SNPs in Table 1, these were genotyped in a subset of 762 discovery stage samples (181 MMR-related febrile seizure cases, 202 MMR-unrelated febrile seizure cases, 379 controls) using KASP assays. The concordance between observed allele counts and imputed allele dosages was high (all six SNPs had $r^2 > 0.96$) indicating that imputation was accurate for these SNPs.

Association Analysis

We used logistic regression to test for differences in allele dosages between cases and controls under an additive genetic model. We carried out combined analysis of the discovery and replication stage data using the inverse variance method applying genomic control⁶¹ to the discovery stage results. Genomic inflation factors were 1.01, 1.00, 1.02, and 1.03 for the four scans (MMR-related febrile seizures versus controls; MMR-related febrile seizures versus MMR-unrelated febrile seizures; MMR-unrelated febrile seizures versus controls; and febrile seizures overall versus controls), respectively, indicating minimal population stratification. In line with this, association results were essentially unchanged when adjusting for the first five principal components from our principal components analysis. We therefore report results where test statistics were scaled by genomic control using the genomic inflation factors, but where no further adjustment was made based on principal components. We estimated heterogeneity between discovery and replication results using the I^2 statistic⁶². In order to explore possible allelic heterogeneity, we conducted analyses conditioning on the top SNP at each of the selected loci. Using the combined discovery and replication data, we tested for interaction effects between the two loci associated with febrile

seizures following MMR vaccination and also between the four loci associated with febrile seizures in general by including risk allele count at each locus in a logistic regression model together with pairwise interaction terms. We evaluated the combined impact of the associated loci by constructing genetic risk scores for all individuals in the discovery and replication samples. For each SNP, a weight ($\log(\text{OR})$) was multiplied by the number (or dosage) of risk alleles. The genetic risk scores were then calculated by summation over the two SNPs associated with MMR-related febrile seizures, or by summation over the four SNPs associated with febrile seizures overall. We used the weighted risk scores in logistic regression analyses. The association analyses were conducted using SNPTEST, METAL⁶³, and R (<http://www.r-project.org/>) software.

Power analysis

For each of the four scans, we estimated the power of the discovery sample at a significance threshold of $P < 1 \times 10^{-6}$ (Supplementary Table 8), since this threshold was used to select SNPs for replication genotyping (Supplementary Fig. 3). Power estimates are presented at representative and relevant odds ratios (ORs) (OR = 1.25, OR = 1.4, OR = 1.5 and OR = 2.0) and risk allele frequencies (0.05, 0.20, 0.30, 0.40 and 0.70). The power analyses were performed using the Genetic Power Calculator⁶⁴.

Bioinformatics analysis

For each locus with genome-wide significant SNPs, we explored possible functional effects of the associations by considering all genotyped or imputed variants with $P < 1 \times 10^{-5}$ at the locus. We searched the National Human Genome Research Institute (NHGRI) GWAS catalog (www.genome.gov/gwastudies) and the National Center for Biotechnology Information (NCBI) Genotype-Tissue Expression (GTEx) database (<http://www.ncbi.nlm.nih.gov/gtex/GTEX2/gtex.cgi>) for previously reported trait or eQTL associations for these variants using P value thresholds of 5×10^{-8} and 1×10^{-4} , respectively. Furthermore, we searched the blood eQTL browser¹² (<http://genenetwork.nl/bloodeqtlbrowser>) for cis and trans eQTL associations in peripheral blood, and the GEUVADIS data browser¹¹ (<http://www.ebi.ac.uk/Tools/geuvadis-das>) for exon and transcript level eQTL associations in lymphoblastoid cell lines. Ensembl (release 74; <http://www.ensembl.org>) IDs were used for annotation of transcripts. MutationTaster⁶⁵ and PolyPhen-2⁶⁶ were used to predict deleteriousness of missense mutations.

Cell-based assays

Assays to assess the impact of ectopic ISG expression on virus infection have been described previously^{14, 67}. Briefly, SCRPSY lentiviral vectors (provided by P. Bieniasz) were used to express the IFI44L variants or an empty cassette as control. Lentiviral-transduced *STAT1*^{-/-} fibroblasts (originally from the lab of J.-L. Casanova) were infected with 1.0 MOI Edmonston strain measles-GFP (provided by R. Cattaneo)⁶⁸. Cells were harvested 24 h post-infection and the percentage of infected cells was quantified by flow cytometry. Tests for mycoplasma contamination of the cells were conducted on multiple occasions (before and after completion of the experiments) and were all negative.

Brain slice preparation

Tmem16C knockout rats and wild-type litter mates were bred at University of California, San Francisco (UCSF) as reported previously³³, and used for whole-cell patch-clamp recordings; they were maintained under a 12:12 hour light/dark schedule, and they consumed food and water *ad libitum*. All protocols were approved by the IACUC at UCSF, and are fully compliant with NIH guidelines for humane treatment of animals.

Postnatal day 10–14 rats were anesthetized with isoflurane and decapitated. Brains were removed and submerged in ice-cold sucrose slicing solution (in mM): 2.5 KCl, 10 MgSO₄·7H₂O, 0.5 CaCl₂·2H₂O, 1.25 NaH₂PO₄·H₂O, 26 NaHCO₃, 11 glucose, 234 sucrose, pH 7.2–7.4, saturated with 95% O₂/5% CO₂. 350- μ m-thick coronal slices containing anterior hypothalamic nucleus (AHN) or hippocampal CA1 neurons were prepared using Leica VT1000s vibratome and transferred to a holding chamber containing artificial cerebral spinal fluid (ACSF, in mM): 126 NaCl, 2.5 KCl, 2 MgCl₂, 2 CaCl₂, 1.25 NaH₂PO₄, 26 NaHCO₃, 10 glucose, pH 7.2–7.4 saturated with 95% O₂/5% CO₂ at 37°C for 20 min for the slices to recover from the treatment in the ice-cold solution, and further incubated for at least 1 hour at room temperature before recording at various temperatures.

Electrophysiology

Whole-cell patch electrodes had pipette tip resistances of 4–6 M Ω , and were filled with a solution containing (in mM): 122 K-gluconate, 13 KCl, 0.07 CaCl₂, 1.0 MgCl₂, 0.1 EGTA, 10.0 HEPES, 4.0 Na-ATP, 0.4 Na-GTP, pH 7.3, and osmolality 290–300 mOsm/L. Recordings were performed using a Multiclamp 700B amplifier (Molecular Devices, Sunnyvale, CA). Signals were sampled at 10 kHz, low-pass filtered at 10 kHz using a Digidata 1440 digitizer, and stored on computer for subsequent analyses using pClamp software (Molecular Devices, Sunnyvale, CA). Liquid junction potential was corrected in reported results. In patch-clamp recordings, access resistance (<15 M Ω) was continuously monitored throughout each experiment. If the fluctuation deviated more than 20% from the baseline values, the cell was regarded as unhealthy or unsuccessful patch, and the recording was excluded. The investigators were blinded to the host animal's genotype while performing electrophysiological recordings.

Whole-cell patch recording was initiated by breaking into the cell under current-clamp mode, followed with current-steps (duration 400 ms) from –100 pA to 120 pA, with a 20 pA increment; the basic membrane properties (at 36.5°C for AHN neurons; at room temperature, 36.5°C, and 40°C for hippocampal neurons) including resting membrane potential (V_m), input resistance (R_{in}), membrane capacitance (C_m) and time constant (τ) were obtained. Specifically, the V_m was obtained directly at holding current 0 pA; R_{in} was determined from the slope of the current-voltage (I–V) relationship at 0 pA holding current by linear regression; τ was determined from the voltage response to –20 pA current injection by exponential regression; C_m was calculated as τ/R_{in} .

In hippocampal recordings, we compared the frequency of action potentials elicited by injection of various amounts of current into wild-type and *Tmem16C* knockout neurons, at room temperature, 36.5°C and 40°C. In hypothalamic recordings, firing rate was monitored

following the shifts of bath temperature between 33°C and 40°C. The bath temperature was controlled using an inline heater (Warner, SC-20). Spontaneous action potentials (SAPs) were counted at the corresponding temperature, and neurons were classified based on their responses: temperature-insensitive neurons have the same frequency of SAP at 33°C, 36.5°C or 40°C; heat-sensitive neurons exhibit a decrease of firing rate during cooling and an increase of SAP firing rate during warming; cold-sensitive neurons show the opposite temperature dependence; silent neurons do not discharge SAPs during the duration of recording.

Fisher's exact test, Student's t-test, or two-way ANOVA followed by Tukey's post-hoc honestly significant difference (HSD) test was used to compare the recordings of wild-type with Tmem16C knockout neurons from the hippocampus and the hypothalamus. All comparisons were based on a sample size of $n > 5$ in line with common practice in single cell electrophysiological recordings.

Supplementary Material

Refer to Web version on PubMed Central for supplementary material.

ACKNOWLEDGMENTS

The study was partially supported by a grant from the Danish Medical Research Council (0602-01818B). Research reported in this publication was supported by National Institutes of Health (NIH)/National Institute of Allergy And Infectious Diseases grant R01AI093697 (A.H.), by NIH/National Institute of Diabetes and Digestive and Kidney Diseases grant K01DK095031 (J.W.S.), and by NIH/National Institute of Neurological Disorders and Stroke grant R01NS069229 (L.Y.J.). The content is solely the responsibility of the authors and does not necessarily represent the official views of the NIH. The Danish National Biobank was established with the support of major grants from the Novo Nordisk Foundation, the Danish Medical Research Council and the Lundbeck Foundation. L.Y.J. is an investigator of the Howard Hughes Medical Institute. B.F. is supported by an Oak Foundation fellowship.

Reference List

1. Barlow WE, et al. The risk of seizures after receipt of whole-cell pertussis or measles, mumps, and rubella vaccine. *N Engl J Med.* 2001; 345:656–661. [PubMed: 11547719]
2. Vestergaard M, et al. MMR vaccination and febrile seizures: evaluation of susceptible subgroups and long-term prognosis. *JAMA.* 2004; 292:351–357. [PubMed: 15265850]
3. Stafstrom, CE. The incidence and prevalence of febrile seizures in. In: Baram, TZ.; Shinnar, S., editors. *Febrile Seizures.* San Diego: Academic Press; 2002.
4. Millichap JG, Millichap JJ. Role of viral infections in the etiology of febrile seizures. *Pediatr. Neurol.* 2006; 35:165–172. [PubMed: 16939854]
5. Helbig I, Scheffer IE, Mulley JC, Berkovic SF. Navigating the channels and beyond: unravelling the genetics of the epilepsies. *Lancet Neurol.* 2008; 7:231–245. [PubMed: 18275925]
6. Poduri A, Lowenstein D. Epilepsy genetics--past, present, and future. *Curr Opin Genet Dev.* 2011; 21:325–332. [PubMed: 21277190]
7. Sadleir LG, Scheffer IE. Febrile seizures. *BMJ.* 2007; 334:307–311. [PubMed: 17289734]
8. Hauser WA, Annegers JF, Anderson VE, Kurland LT. The risk of seizure disorders among relatives of children with febrile convulsions. *Neurology.* 1985; 35:1268–1273. [PubMed: 4022374]
9. Eckhaus J, et al. Genetics of febrile seizure subtypes and syndromes: a twin study. *Epilepsy Res.* 2013; 105:103–109. [PubMed: 23522981]
10. Kjeldsen MJ, Kyvik KO, Friis ML, Christensen K. Genetic and environmental factors in febrile seizures: a Danish population-based twin study. *Epilepsy Res.* 2002; 51:167–177. [PubMed: 12350392]

11. Lappalainen T, et al. Transcriptome and genome sequencing uncovers functional variation in humans. *Nature*. 2013; 501:506–511. [PubMed: 24037378]
12. Westra HJ, et al. Systematic identification of trans eQTLs as putative drivers of known disease associations. *Nat Genet*. 2013; 45:1238–1243. [PubMed: 24013639]
13. Zilliox MJ, Parmigiani G, Griffin DE. Gene expression patterns in dendritic cells infected with measles virus compared with other pathogens. *Proc Natl Acad Sci U S A*. 2006; 103:3363–3368. [PubMed: 16492729]
14. Schoggins JW, et al. A diverse range of gene products are effectors of the type I interferon antiviral response. *Nature*. 2011; 472:481–485. [PubMed: 21478870]
15. Dhiman N, et al. Variations in measles vaccine-specific humoral immunity by polymorphisms in SLAM and CD46 measles virus receptors. *J Allergy Clin Immunol*. 2007; 120:666–672. [PubMed: 17560639]
16. Kennedy RB, et al. Multigenic control of measles vaccine immunity mediated by polymorphisms in measles receptor, innate pathway, and cytokine genes. *Vaccine*. 2012; 30:2159–2167. [PubMed: 22265947]
17. Clifford HD, et al. CD46 measles virus receptor polymorphisms influence receptor protein expression and primary measles vaccine responses in naive Australian children. *Clin Vaccine Immunol*. 2012; 19:704–710. [PubMed: 22357652]
18. Ovsyannikova IG, et al. The association of CD46, SLAM and CD209 cellular receptor gene SNPs with variations in measles vaccine-induced immune responses: a replication study and examination of novel polymorphisms. *Hum Hered*. 2011; 72:206–223. [PubMed: 22086389]
19. Kemper C, et al. Activation of human CD4+ cells with CD3 and CD46 induces a T-regulatory cell 1 phenotype. *Nature*. 2003; 421:388–392. [PubMed: 12540904]
20. Dorig RE, Marcil A, Chopra A, Richardson CD. The human CD46 molecule is a receptor for measles virus (Edmonston strain). *Cell*. 1993; 75:295–305. [PubMed: 8402913]
21. Nanche D, et al. Human membrane cofactor protein (CD46) acts as a cellular receptor for measles virus. *J Virol*. 1993; 67:6025–6032. [PubMed: 8371352]
22. Ono N, et al. Measles viruses on throat swabs from measles patients use signaling lymphocytic activation molecule (CDw150) but not CD46 as a cellular receptor. *J Virol*. 2001; 75:4399–4401. [PubMed: 11287589]
23. Thomas EA, et al. Heat opens axon initial segment sodium channels: a febrile seizure mechanism? *Ann Neurol*. 2009; 66:219–226. [PubMed: 19743470]
24. Heron SE, et al. Sodium-channel defects in benign familial neonatal-infantile seizures. *Lancet*. 2002; 360:851–852. [PubMed: 12243921]
25. Liao Y, et al. Molecular correlates of age-dependent seizures in an inherited neonatal-infantile epilepsy. *Brain*. 2010; 133:1403–1414. [PubMed: 20371507]
26. Schadt EE, et al. Mapping the genetic architecture of gene expression in human liver. *PLoS Biol*. 2008; 6:e107. [PubMed: 18462017]
27. Kasperaviciute D, et al. Epilepsy, hippocampal sclerosis and febrile seizures linked by common genetic variation around SCN1A. *Brain*. 2013; 136:3140–3150. [PubMed: 24014518]
28. Heinzen EL, et al. Nova2 interacts with a cis-acting polymorphism to influence the proportions of drug-responsive splice variants of SCN1A. *Am. J Hum Genet*. 2007; 80:876–883. [PubMed: 17436242]
29. Ogiwara I, et al. Nav1.1 localizes to axons of parvalbumin-positive inhibitory interneurons: a circuit basis for epileptic seizures in mice carrying an *Scn1a* gene mutation. *J Neurosci*. 2007; 27:5903–5914. [PubMed: 17537961]
30. Rossignol E. Genetics and Function of Neocortical GABAergic Interneurons in Neurodevelopmental Disorders. *Neural Plasticity*. 2011
31. Duran C, Hartzell HC. Physiological roles and diseases of Tmem16/Anoctamin proteins: are they all chloride channels? *Acta Pharmacol. Sin*. 2011; 32:685–692. [PubMed: 21642943]
32. Charlesworth G, et al. Mutations in ANO3 cause dominant craniocervical dystonia: ion channel implicated in pathogenesis. *Am. J Hum Genet*. 2012; 91:1041–1050. [PubMed: 23200863]

33. Huang F, et al. TMEM16C facilitates Na(+)-activated K⁺ currents in rat sensory neurons and regulates pain processing. *Nat Neurosci.* 2013; 16:1284–1290. [PubMed: 23872594]
34. Meyer TE, et al. Genome-wide association studies of serum magnesium, potassium, and sodium concentrations identify six Loci influencing serum magnesium levels. *PLoS Genet.* 2010; 6
35. Kruse HD, Orent ER, McCollum EV. Studies on magnesium deficiency in animals I. Symptomatology resulting from magnesium deprivation. *Journal of Biological Chemistry.* 1932; 96:519–539.
36. HANNA S, HARRISON M, MacINTYRE I, FRASER R. The syndrome of magnesium deficiency in man. *Lancet.* 1960; 2:172–176. [PubMed: 14399531]
37. Anderson WW, Lewis DV, Swartzwelder HS, Wilson WA. Magnesium-free medium activates seizure-like events in the rat hippocampal slice. *Brain Res.* 1986; 398:215–219. [PubMed: 3801897]
38. Ghasemi M, Schachter SC. The NMDA receptor complex as a therapeutic target in epilepsy: a review. *Epilepsy Behav.* 2011; 22:617–640. [PubMed: 22056342]
39. Boulant JA. Role of the preoptic-anterior hypothalamus in thermoregulation and fever. *Clin Infect Dis.* 2000; 31(Suppl 5):S157–S161. [PubMed: 11113018]
40. Sugiura Y, Ogiwara I, Hoshi A, Yamakawa K, Ugawa Y. Different degrees of loss of function between GEFS+ and SMEI Nav 1.1 missense mutants at the same residue induced by rescuable folding defects. *Epilepsia.* 2012; 53:e111–e114. [PubMed: 22525008]
41. Martin MS, et al. Altered function of the SCN1A voltage-gated sodium channel leads to gamma-aminobutyric acid-ergic (GABAergic) interneuron abnormalities. *J Biol Chem.* 2010; 285:9823–9834. [PubMed: 20100831]
42. Turner TL, Cockburn F, Forfar JO. Magnesium therapy in neonatal tetany. *Lancet.* 1977; 1:283–284. [PubMed: 64807]
43. Euser AG, Cipolla MJ. Magnesium sulfate for the treatment of eclampsia: a brief review. *Stroke.* 2009; 40:1169–1175. [PubMed: 19211496]
44. Yuen AW, Sander JW. Can magnesium supplementation reduce seizures in people with epilepsy? A hypothesis. *Epilepsy Res.* 2012; 100:152–156. [PubMed: 22406257]
45. Abdelmalik PA, Politzer N, Carlen PL. Magnesium as an effective adjunct therapy for drug resistant seizures. *Can J Neurol. Sci.* 2012; 39:323–327. [PubMed: 22547512]
46. Barcia G, et al. De novo gain-of-function KCNT1 channel mutations cause malignant migrating partial seizures of infancy. *Nat Genet.* 2012; 44:1255–1259. [PubMed: 23086397]
47. Heron SE, et al. Missense mutations in the sodium-gated potassium channel gene KCNT1 cause severe autosomal dominant nocturnal frontal lobe epilepsy. *Nat Genet.* 2012; 44:1188–1190. [PubMed: 23086396]
48. Wray NR, Purcell SM, Visscher PM. Synthetic associations created by rare variants do not explain most GWAS results. *PLoS. Biol.* 2011; 9:e1000579. [PubMed: 21267061]
49. Tsuboi T. Epidemiology of febrile and afebrile convulsions in children in Japan. *Neurology.* 1984; 34:175–181. [PubMed: 6538005]
50. Lynge E, Sandegaard JL, Rebolj M. The Danish National Patient Register. *Scand J Public Health.* 2011; 39:30–33. [PubMed: 21775347]
51. Vestergaard M, et al. The Danish National Hospital Register is a valuable study base for epidemiologic research in febrile seizures. *J Clin Epidemiol.* 2006; 59:61–66. [PubMed: 16360562]
52. Knudsen LB, Olsen J. The Danish Medical Birth Registry. *Dan. Med Bull.* 1998; 45:320–323. [PubMed: 9675544]
53. Hviid A. Postlicensure epidemiology of childhood vaccination: the Danish experience. *Expert. Rev Vaccines.* 2006; 5:641–649. [PubMed: 17181438]
54. Olsen J, et al. The Danish National Birth Cohort--its background, structure and aim. *Scand. J. Public Health.* 2001; 29:300–307. [PubMed: 11775787]
55. Pedersen CB, Gotzsche H, Moller JO, Mortensen PB. The Danish Civil Registration System. A cohort of eight million persons. *Dan. Med. Bull.* 2006; 53:441–449. [PubMed: 17150149]

56. Hollegaard MV, et al. Genome-wide scans using archived neonatal dried blood spot samples. *BMC. Genomics*. 2009; 10:297. [PubMed: 19575812]
57. A map of human genome variation from population-scale sequencing. *Nature*. 2010; 467:1061–1073. [PubMed: 20981092]
58. Delaneau O, Marchini J, Zagury JF. A linear complexity phasing method for thousands of genomes. *Nat Methods*. 2012; 9:179–181. [PubMed: 22138821]
59. Howie BN, Donnelly P, Marchini J. A flexible and accurate genotype imputation method for the next generation of genome-wide association studies. *PLoS Genet*. 2009; 5:e1000529. [PubMed: 19543373]
60. Marchini J, Howie B. Genotype imputation for genome-wide association studies. *Nat. Rev. Genet*. 2010; 11:499–511. [PubMed: 20517342]
61. Devlin B, Roeder K. Genomic control for association studies. *Biometrics*. 1999; 55:997–1004. [PubMed: 11315092]
62. Higgins JP, Thompson SG. Quantifying heterogeneity in a meta-analysis. *Stat. Med*. 2002; 21:1539–1558. [PubMed: 12111919]
63. Willer CJ, Li Y, Abecasis GR. METAL: fast and efficient meta-analysis of genomewide association scans. *Bioinformatics*. 2010; 26:2190–2191. [PubMed: 20616382]
64. Purcell S, Cherny SS, Sham PC. Genetic Power Calculator: design of linkage and association genetic mapping studies of complex traits. *Bioinformatics*. 2003; 19:149–150. [PubMed: 12499305]
65. Schwarz JM, Rodelsperger C, Schuelke M, Seelow D. MutationTaster evaluates disease-causing potential of sequence alterations. *Nat Methods*. 2010; 7:575–576. [PubMed: 20676075]
66. Adzhubei IA, et al. A method and server for predicting damaging missense mutations. *Nat Methods*. 2010; 7:248–249. [PubMed: 20354512]
67. Schoggins JW, et al. Dengue reporter viruses reveal viral dynamics in interferon receptor-deficient mice and sensitivity to interferon effectors in vitro. *Proc Natl Acad Sci U S A*. 2012; 109:14610–14615. [PubMed: 22908290]
68. Dupuis S, et al. Impaired response to interferon-alpha/beta and lethal viral disease in human STAT1 deficiency. *Nat Genet*. 2003; 33:388–391. [PubMed: 12590259]

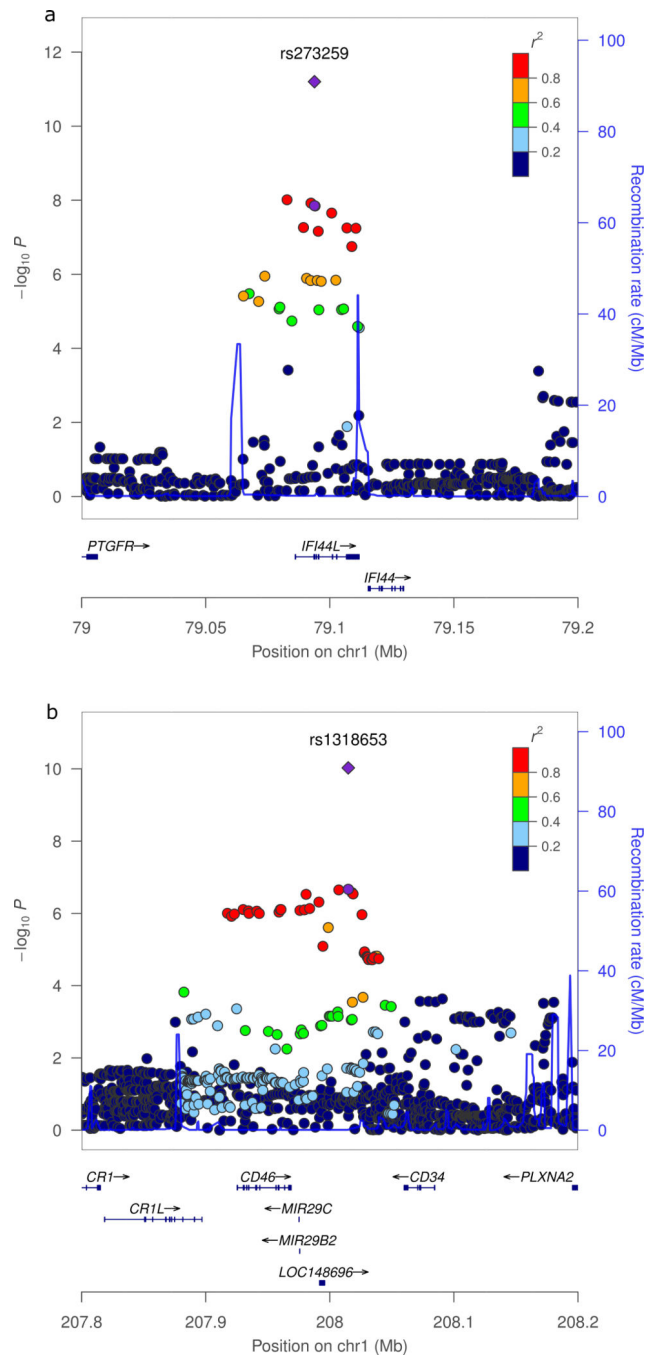


Figure 1. Discovery stage results from the MMR-related febrile seizures versus controls scan. **(a, b)** Regional association plots for the **(a)** 1p31.1 locus, and **(b)** 1q32.2 locus. SNPs are plotted by chromosomal location (x-axis) and disease association ($-\log_{10} P$ value; left y-axis). The colors reflect linkage disequilibrium of each SNP with the top SNP at the locus, and recombination rates (from HapMap; right y-axis) are shown to reflect local linkage disequilibrium structure. The P value for the top SNP in the combined analysis is

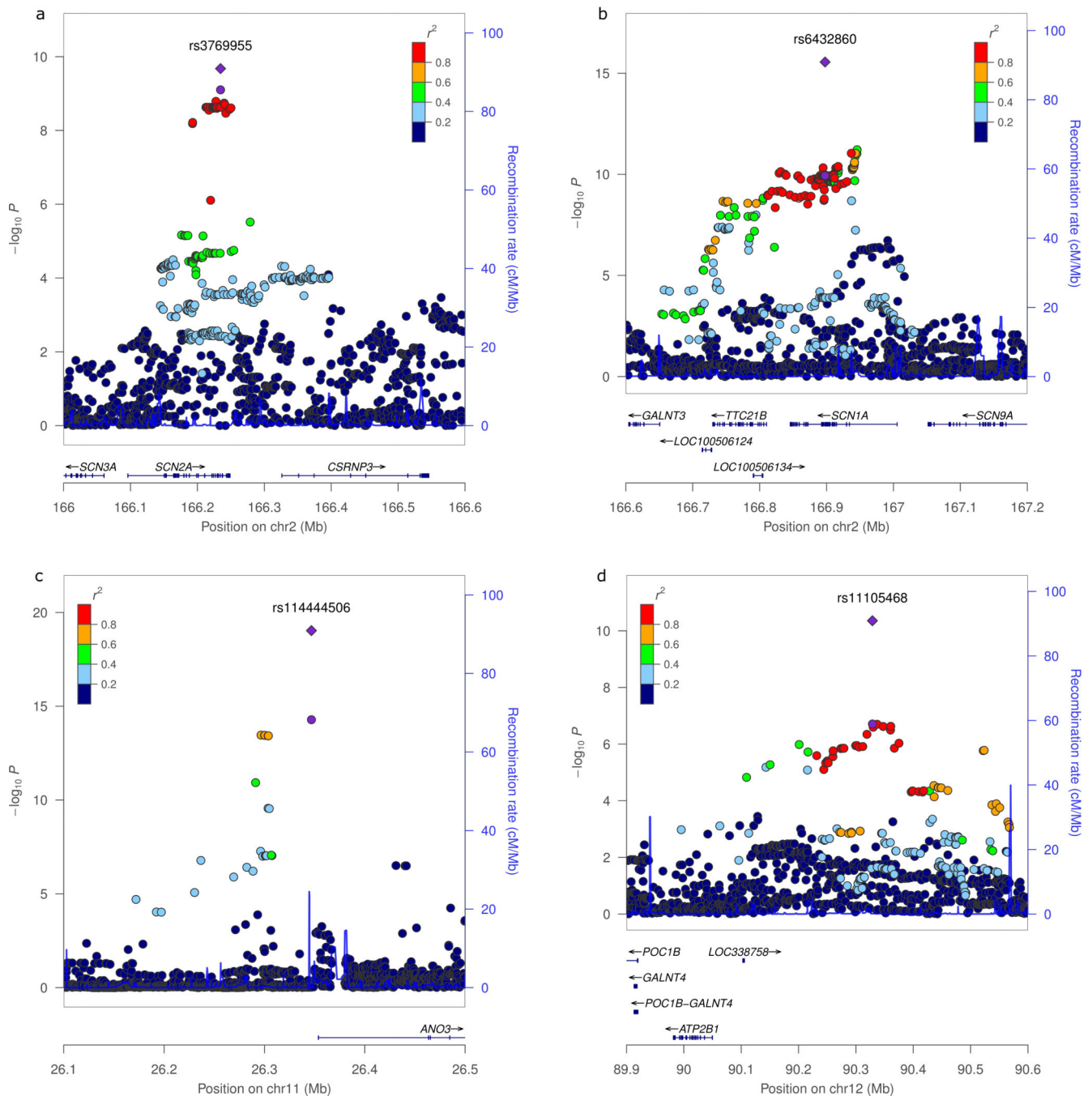
represented by a purple diamond, and that from the discovery stage analysis by a purple circle.

Author Manuscript

Author Manuscript

Author Manuscript

Author Manuscript

**Figure 2.**

Discovery stage results from the febrile seizures overall versus controls scan. **(a–d)** Regional association plots for the **(a)** 2q24.3 (*SCN2A*) locus, **(b)** 2q24.3 (*SCN1A*) locus, **(c)** 11p14.2 locus, and **(d)** 12q21.33 locus. SNPs position (x-axis) and disease association ($-\log_{10} P$ value; left y-axis) are shown, and the colors reflect linkage disequilibrium of each SNP with the top SNP at the locus. Recombination rates are from HapMap (right y-axis). The P value for the top SNP in the combined analysis is represented by a purple diamond, and that from the discovery stage analysis by a purple circle.

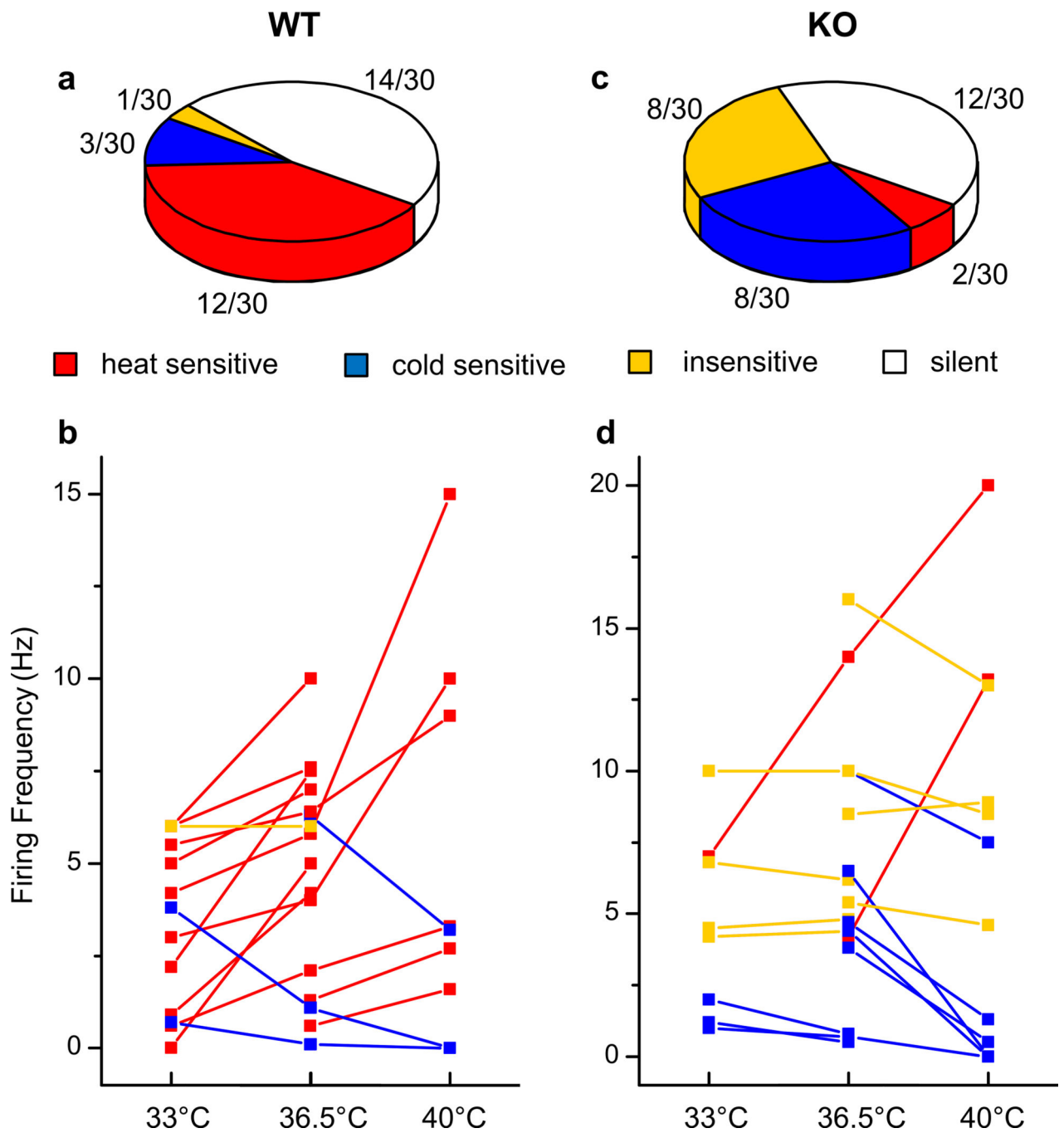


Figure 3. *TMEM16C* is involved in hypothalamic neurons' temperature response. Neurons in the anterior hypothalamic nucleus (AHN) were classified based on their temperature responses as heat-sensitive (red), cold-sensitive (blue), temperature-insensitive (light orange), or silent (white). Proportion of each type of neurons in AHN from (a) wild-type (WT) or (c) knockout (KO) rats. Firing frequencies of each individual neurons from (b) WT or (d) KO rats recorded at 33°C, 36.5°C or 40°C. A lower proportion of heat-sensitive neurons were

detected in *Tmem16C* knockout slices ($n = 30$ recorded neurons), compared with wild-type ($n = 30$; $P = 0.005$, Fisher's exact test).

Author Manuscript

Author Manuscript

Author Manuscript

Author Manuscript

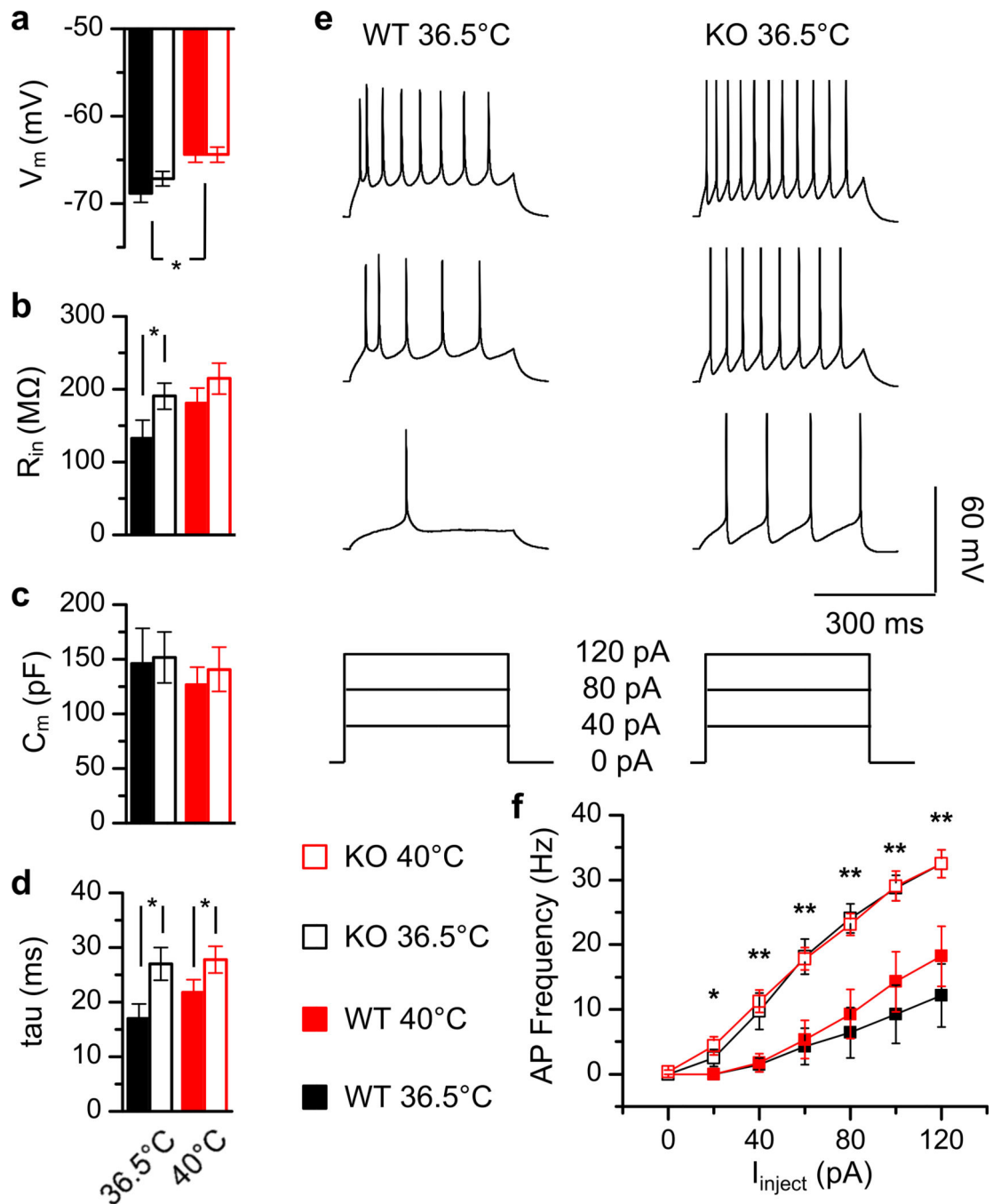


Figure 4.

Hippocampal CA1 pyramidal neurons exhibit hyperexcitability in the absence of *TMEM16C*. (**a-d**) Basic membrane properties (*, $P < 0.05$, two-way ANOVA followed by HSD test), namely (**a**) resting membrane potential (V_m), (**b**) input resistance (R_{in}), (**c**) membrane capacitance (C_m) and (**d**) time constant (τ) at 36.5°C and 40°C, for wild-type (WT) vs., *Tmem16C* knockout (KO) neurons ($n = 7-8$). (**e**) Sample traces of neuronal responses to 40, 80, and 120 pA current injections in wild-type vs. knockout CA1 pyramidal neurons at 36.5°C. (**f**) Current-steps elicit more action potentials in knockout neurons

compared to wild-type controls ($n = 7-8$; **, $P < 0.01$, *, $P < 0.05$, WT vs. KO, two-way ANOVA). Error bars indicate s.e.m.

Author Manuscript

Author Manuscript

Author Manuscript

Author Manuscript

Table 1

Discovery, replication and combined results for six loci associated with febrile seizures following MMR vaccination and overall. Results with $P < 1.25 \times 10^{-8}$ are marked in bold. “MMR+” represents MMR-related febrile seizure cases and “MMR-” represents MMR-unrelated febrile seizure cases. “Ctrls” in the MMR-related vs. unrelated febrile seizure analyses are febrile seizure cases unrelated to MMR vaccination. Ctrls, controls. CI, confidence interval. FS, febrile seizures., I^2 , heterogeneity estimate., P_{het} , P value from Cochran Q test of heterogeneity.

Chromosome Position (bp)	SNP (effect/alternative allele)	Analysis	Discovery			Replication			Combined					
			Effect Allele frequency	Cases	Ctrls	Odds Ratio (95% CI)	P	Effect Allele Frequency	Cases	Ctrls	Odds Ratio (95% CI)	P	I^2	P_{het}
<i>Loci for MMR-related FS</i>														
1	79093818 rs273259 A/G	MMR+ vs ctrls	0.767	0.702	1.40 (1.25–1.57)	1.4×10^{-8}	0.754	0.683	1.42 (1.19–1.69)	9.2×10^{-5}	1.41 (1.28–1.55)	5.9×10^{-12}	0	0.91
		MMR+ vs MMR-	0.767	0.694	1.46 (1.26–1.69)	2.0×10^{-7}	0.754	0.692	1.36 (1.13–1.64)	0.00096	1.42 (1.27–1.59)	1.2×10^{-9}	0	0.57
		MMR- vs ctrls	0.694	0.702	0.97 (0.87–1.07)	0.52	0.692	0.683	1.04 (0.92–1.17)	0.53	1.00 (0.92–1.08)	0.95	0	0.36
		All FS vs ctrls	0.728	0.702	1.14 (1.05–1.24)	0.0027	0.709	0.683	1.13 (1.01–1.26)	0.028	1.14 (1.06–1.21)	0.0002	0	0.91
1	208014922 rs1318653 T/C	MMR+ vs ctrls	0.828	0.774	1.41 (1.24–1.60)	2.1×10^{-7}	0.831	0.767	1.49 (1.22–1.82)	8.8×10^{-5}	1.43 (1.28–1.59)	9.6×10^{-11}	0	0.64
		MMR+ vs MMR-	0.828	0.771	1.44 (1.23–1.68)	5.9×10^{-6}	0.831	0.761	1.55 (1.25–1.91)	4.1×10^{-5}	1.48 (1.30–1.67)	1.6×10^{-9}	0	0.59
		MMR- vs ctrls	0.771	0.774	0.98 (0.87–1.10)	0.74	0.761	0.767	0.96 (0.85–1.10)	0.58	0.97 (0.89–1.06)	0.54	0	0.84
		All FS vs ctrls	0.797	0.774	1.15 (1.05–1.26)	0.0037	0.781	0.767	1.08 (0.96–1.22)	0.22	1.12 (1.04–1.21)	0.0023	0	0.41
<i>Loci for FS overall</i>														
2	166234632 rs3769955 (T/C)	MMR+ vs ctrls	0.455	0.4	1.26 (1.13–1.39)	1.4×10^{-5}	0.451	0.417	1.15 (0.99–1.34)	0.076	1.22 (1.12–1.33)	4.2×10^{-6}	0	0.35
		MMR+ vs MMR-	0.455	0.462	0.97 (0.86–1.10)	0.64	0.451	0.444	1.03 (0.87–1.21)	0.74	0.99 (0.90–1.09)	0.87	0	0.59

Author Manuscript

Author Manuscript

Author Manuscript

Author Manuscript

Chromosome Position (bp) SNP (effect/alternative allele)	Analysis	Discovery (MMR-related FS, <i>n</i> = 929, MMR-unrelated FS, <i>n</i> = 1,070, FS overall, <i>n</i> = 1,999, Controls, <i>n</i> = 4,118)			Replication (MMR-related FS, <i>n</i> = 405 to 408, MMR-unrelated FS, <i>n</i> = 1,030 to 1,034, FS overall, <i>n</i> = 1,435 to 1,442, Controls, <i>n</i> = 1,625 to 1,645)			Combined (MMR-related FS, <i>n</i> = 1,334 to 1,337, MMR-unrelated FS, <i>n</i> = 2,100 to 2,104, FS overall, <i>n</i> = 3,434 to 3,441, Controls, <i>n</i> = 5,743 to 5,863)					
		Effect Allele frequency		Odds Ratio	Effect Allele Frequency		Odds Ratio	Odds Ratio					
		Cases	Ctrls	(95% CI)	Cases	Ctrls	(95% CI)	<i>P</i>	<i>I</i> ²	<i>P</i> _{het}			
2 166897864 rs6432860 (G/A)	MMR- vs ctrls	0.462	0.4	1.30 (1.17-1.43)	2.1 × 10 ⁻⁷	0.444	0.417	1.12 (1.00-1.25)	0.047	1.22 (1.13-1.31)	1.9 × 10 ⁻⁷	73	0.05
	All FS vs ctrls	0.459	0.4	1.28 (1.18-1.38)	7.9 × 10 ⁻¹⁰	0.446	0.417	1.13 (1.02-1.25)	0.02	1.22 (1.15-1.30)	3.1 × 10 ⁻¹⁰	72	0.06
11 26346831 rs114444506 (C/T)	MMR+ vs ctrls	0.777	0.704	1.48 (1.31-1.66)	1.0 × 10 ⁻¹⁰	0.754	0.709	1.26 (1.06-1.50)	0.01	1.41 (1.27-1.55)	1.0 × 10 ⁻¹¹	53	0.14
	MMR+ vs MMR-	0.777	0.744	1.20 (1.04-1.39)	0.014	0.754	0.771	0.91 (0.75-1.10)	0.33	1.08 (0.96-1.22)	0.18	80	0.02
	MMR- vs ctrls	0.744	0.704	1.22 (1.10-1.36)	0.00024	0.771	0.709	1.38 (1.22-1.57)	5.6 × 10 ⁻⁷	1.29 (1.19-1.40)	1.7 × 10 ⁻⁹	52	0.15
	All FS vs ctrls	0.76	0.704	1.33 (1.22-1.45)	1.2 × 10 ⁻¹⁰	0.767	0.709	1.35 (1.20-1.51)	3.4 × 10 ⁻⁷	1.34 (1.25-1.43)	2.2 × 10 ⁻¹⁶	0	0.87
12 90328833 rs11105468 (A/T)	MMR+ vs ctrls	0.06	0.028	2.26 (1.76-2.89)	1.1 × 10 ⁻¹⁰	0.049	0.028	1.81 (1.24-2.64)	0.002	2.11 (1.72-2.60)	1.5 × 10 ⁻¹²	0	0.34
	MMR+ vs MMR-	0.06	0.055	1.11 (0.84-1.46)	0.46	0.049	0.054	0.91 (0.63-1.32)	0.61	1.03 (0.83-1.29)	0.77	0	0.4
	MMR- vs ctrls	0.055	0.028	2.07 (1.62-2.64)	5.0 × 10 ⁻⁹	0.054	0.028	1.99 (1.50-2.64)	1.3 × 10 ⁻⁶	2.03 (1.69-2.45)	4.8 × 10 ⁻¹⁴	0	0.83
	All FS vs ctrls	0.058	0.028	2.18 (1.79-2.64)	5.2 × 10 ⁻¹⁵	0.052	0.028	1.94 (1.49-2.52)	6.9 × 10 ⁻⁷	2.09 (1.79-2.44)	3.7 × 10 ⁻²⁰	0	0.49
MMR+ vs ctrls	0.342	0.292	1.26 (1.13-1.40)	3.2 × 10 ⁻⁵	0.359	0.296	1.33 (1.14-1.57)	0.0005	1.28 (1.17-1.40)	6.5 × 10 ⁻⁸	0	0.56	
	0.342	0.338	1.02 (0.90-1.16)	0.76	0.359	0.339	1.09 (0.92-1.29)	0.31	1.05 (0.94-1.16)	0.39	0	0.54	
	0.338	0.292	1.23 (1.11-1.36)	7.6 × 10 ⁻⁵	0.339	0.296	1.22 (1.08-1.37)	0.0009	1.23 (1.14-1.33)	2.4 × 10 ⁻⁷	0	0.92	
All FS vs ctrls	0.34	0.292	1.24 (1.15-1.35)	2.0 × 10 ⁻⁷	0.345	0.296	1.25 (1.12-1.39)	3.9 × 10 ⁻⁵	1.25 (1.17-1.33)	3.4 × 10 ⁻¹¹	0	0.92	